ISSN: 2454-9940

INTERNATIONAL JOURNAL OF APPLIED SCIENCE ENGINEERING AND MANAGEMENT

E-Mail :
editor.ijasem@gmail.com
editor@ijasem.org

www.ijasem.org

INTERNATIONAL JOURNAL OF APPLIED SCIENCE ENGINEERING AND MANAGEMENT

ISSN2454-9940www.ijsem.org

Vol 7, Issuse.4 Oct 2019

Higher-order slip characteristics, activation energy, and bioconvection in Reiner–Philippoff nanofluid flow were studied numerically.

Dhanujaya Rao Kodali [1],Dr.Kummari Srinicas[2],Mohamad Jahangir Pasha[3],Manchala Ramesh [4],

ABSTRACT

Research into nanofluids' enhanced thermal mechanisms, which may be used in heat transfer devices, cooling procedures, and energy generation, is the most exciting. Their significance in biomedical engineering and biotechnology is shown by nanofluids containing mobile microorganisms. Reiner–Philippoff nanofluid's accessible dynamic property is shown in this study using bioconvection applications. The magnetic force impact and activation energy properties of Reiner–Philippoff nanomaterial are also meant to undertake radiative analysis. To better understand the flow, higher-order relations are included in the slip. Thermal radiation with a nonlinear connection is used to propose changes to the energy equation. In order to solve the flow equations numerically, a shooting system is used. Analysis of the recommended parameters is provided in full. In order to study the variation in heat, mass and motile density function, numerical data is obtained With Philippoff fluid parameter, velocity profile improves but slip parameter decreases in the simulations. Temperature and concentration profiles decreased when the Philippoff fluid parameter was raised. Higher order slip is more efficient in boosting temperature, concentration, and the profiles of microorganisms.

Introduction

Nanofluids are well-known materials with innovative thermal uses in a wide range of engineering and industrial fields, as well as in numerous scientific epochs. Before certain dynamic applications in heating and cooling devices, nuclear heating and cooling devices, solar problems and magnetic retention, astronomy and safety and automated operation can be considered, nanofluids' thermophysical features must be considered. Nanoparticles are often thought of being metallic specks less than 100 nm in size. Nanofluids, unlike typical viscous liquids, are more efficient at transferring energy. Until now, nanofluids have not been studied from a thermal standpoint. These tiny nanofluids were studied by Buongiorno2 for their thermophoretic and Brownian motion. The Buongiorno model is used to illustrate the stability of nanomaterials due to Brownian and thermophoretic effects. Stagnation point phenomena affect the melting characteristics of Jeffrey nanofluid flow, which was studied by Chakraborty et al3. An extra magnetic force was added to the nanofluid issue to account for the slip characteristics. For Jeffrey nanofluid flow with a mixed convection source, Gul et al. designed an analysis that transmitted the most efficient analysis. 5 Corresponding author Ahmed et al.6 employed nanofluid. Contact information: mmbhatti at sdust.edu.cn e-mail (M.M. Bhatti). See how a verticle cylinder limits entropy formation. The dissipation characteristics of Williamson nanofluid between spinning discs were studied by Qayyum et al.7. While investigating the thermal assignment of micropolar nanofluids for cooling and heating applications, Turkyilma zoglu8 was able to correctly calculate the precise answer. In the three-dimensional investigation of Prandtl nanofluid, the involvement of higher-order chemical processes was envisioned. As a result of the theoretical nanofluid focused by Rashidis et al.10, the thermal characteristics of a convectively heated isothermal surface were evaluated. In the three-dimensional movement of nanofluids with electromagnetic and radiation applications, Amel et al.11 examined the Joule heating and slipping viewpoint. When slip effects dominate, Ibrahim12 calculated the thermal improvement of tangent hyperbolic nanofluid.

Dept.: Humanities & Science
Pallavi Engineering College,
Kuntloor(V),Hayathnagar(M),Hyderabad,R.R.Dist.-501505

For nanofluid flow in a microchannel with porous walls, Khan et al.13 investigated the interfacial electrokinetic process. In a porous region, Waqas et al.14 used a numerical framework to guide the combined rheological effects of Maxwell and micropolar nanofluid. Optimized nanofluid flow owing to heated substrate was carried out by Adesanya et al.15. The blood flow of nanoparticles was studied by Seikh et al.16 in relation to the slip characteristics and magnetic force. The thermal radiation and convective bound ary conditions characteristics for Carreau and Casson nanofluid flow over stretched surface were addressed by Mahan thesh et al.17 in their paper published in Nature Communications. The bioconvection method relies on microorganisms with lower densities floating in the water. Due of the non-uniform instability structure, microorganisms typically swim in the top zone. Because of the increased stratification density, the top area becomes unstable due to the swimming of these biological microorganisms on the upper surface. In microfluidic applications, the interaction between bioconvection and nanoparticles seems to be crucial because the uniform motion of nanoparticles is free from the movement of swimming microorganisms. Kuznetsov made a substantial contribution to the bioconvection phenomena with nanofluid flow.18 Using gyrotactic microorganisms and a truncated cone, Khan et al.19 investigated the convective transport of nanofluid. For the stability and heat increase of nanofluids with magnetic force characteristics, Al-Hussain et al.20 said that bioconvection was critical. Nanomaterial bioconvection evaluation over Riga design is illustrated by Zaffar et al. numerical benchmark. 21 Carreau nanofluid containing motile microbes was studied by Elayarani et al.22. Microorganisms have an important role in three-dimensional cross-nanofluid flow, according to Hosseinzadeh et al.23. Walters-bio-convective B's nanofluid model issue was studied by Khan et al.24 using an analytical approach. nonlinear mixed convection is included into this model. By Tlili et al., researchers have tackled the twofold stratification bioconvection study of the micropolar nanofluid flow under the slip mechanism. 25 Microorganisms and a magnetic dipole were used to explain the thermal process of ferromagnets using microorganisms and a magnetic dipole. Bioconvection has been used in nanofluid flow in the presence of higher-order slip and activation energy in Reiner–Philippon flow. Nonlinear radiation relations are used to address Reiner–Philippoff nanofluid thermal applications. This nanofluid has unique thermal properties compared to other non-Newtonian models. 27–30 When higher-order slip relations are used, two useful slip parameters are generated, allowing the transport process to be controlled. Nonlinear equations are numerically validated using a firing strategy.

Mathematical modeling

If you want to know how to simulate nanofluids and gyrotactic bacteria when the slip perspective is more prevalent, this section is for you. Discussing two-dimensional flow, the steady and incompressible flow assumptions are kept in mind (see Fig. A). The Buongiorno model reveals the Brownian and thermophoretic individuality of the system. With u and v taken in opposite directions, the surface is stretched in the direction of flow while u is opposed along the sheet. The flow direction is generally dictated by the magnetic force. There is a consensus that the flow domain has a uniform nanofluid temperature, concentration, and motile density (T, C, and N). The energy equation is tweaked using special relations for thermally radiative flow analysis. A non-Newtonian fluid model in three dimensions, the Reiner– Philippoff fluid is so called. Models like this show the low and high shear rates that restrict viscosity, which is intriguing. Viscosity and shear rate must be increased to reach the typical findings for viscous fluids. Furthermore, at = 0, values for viscous fluid are obtained at = 0.. Between these two levels of viscosity, the Reiner–Philippoff fluid has a non-Newtonian character. With deformation rate (u y) and shear stress (), the shear stress and deformation rate relations of the Reiner–Philippoff fluid model are defined as27–30: The governing equations for the issue under consideration are 26–

30:

$$\frac{\partial u}{\partial x}+\frac{\partial u}{\partial y}=0, \tag{2.2}$$

$$u\frac{\partial u}{\partial x}+v\frac{\partial u}{\partial y} = \frac{1}{\rho_f}\frac{\partial \tau}{\partial y}-\frac{\sigma_c B_0^2}{\rho_f} + \frac{g_1}{\rho_f}\begin{bmatrix}\left(1-C_f\right)\rho_f\beta^*\left(T-T_\infty\right)-\left(\rho_p-\rho_f\right)\left(C-C_\infty\right)\\ -\left(N-N_\infty\right)\gamma^*\left(\rho_m-\rho_f\right)\end{bmatrix}, \tag{2.3}$$

$$u\frac{\partial T}{\partial x}+v\frac{\partial T}{\partial y}=\Lambda_f\frac{\partial^2 T}{\partial y^2}+\frac{16\sigma^*}{3(\rho c)_f\kappa^*}\frac{\partial}{\partial y}\left(T^3\frac{\partial T}{\partial y}\right) + \frac{\left(\rho c_p\right)_p}{\left(\rho c_p\right)_f}\left[D_B\left(\frac{\partial C}{\partial y}\frac{\partial T}{\partial y}\right)+\frac{D_T}{T_\infty}\left(\frac{\partial T}{\partial y}\right)^2\right], \tag{2.4}$$

$$u\frac{\partial C}{\partial x}+v\frac{\partial C}{\partial y}=D_B\frac{\partial^2 C}{\partial y^2}+\frac{D_T}{T_\infty}\frac{\partial^2 T}{\partial y^2}-Kr^2\left(C-C_\infty\right)\left(\frac{T}{T_\infty}\right)^n\exp\left(\frac{-E_a}{k_1 T}\right), \tag{2.5}$$

$$u\frac{\partial N}{\partial x}+v\frac{\partial N}{\partial y}+\frac{\hat{b}\hat{w}}{\left(C_w-C_\infty\right)}\left[\frac{\partial}{\partial y}\left(N\frac{\partial C}{\partial y}\right)\right]=D_m\frac{\partial^2 N}{\partial y^2}, \tag{2.6}$$

The Rosseland approximations are used to include nonlinear thermal relations into the energy equation for radiative phenomena. Eq. (2.5) also includes the activation energy, which is calculated using the Arrhenius equations in the final component of the equation. The parameters are as follows:

$$u=u_w(x)=ax^{\frac{1}{3}}+u_{slip},\ u_{slip}=A\frac{\partial u}{\partial y}+B\frac{\partial^2 u}{\partial y^2},\ v=0,$$

$$-k\frac{\partial T}{\partial y}=h_f\left(T_f-T\right),\ D_B\frac{\partial C}{\partial y}+\frac{D_T}{T_\infty}\frac{\partial T}{\partial y},\ N=N_w,\quad at\quad y=0,$$

Physical quantities such as f (fluid density), c (electrical conductivity), B0 (magnetic field strength), physical quantities such as f (fluid density), cp (nanoparticles heat capacity), w (swimming cells speed), (volume suspension coefficient), DB (diffusion constant), b (chemo taxis constant), k (mean absorption coefficient), Dm (microorganisms diffusion constant), g (gravity), (cp) p (nanofluid density) For the present flow model, the following non-dimensional expressions are expected: :

$$\left.\begin{aligned}&\eta=\sqrt{\frac{a}{v}}\frac{y}{x^{\frac{1}{3}}},\psi=\sqrt{avx}^{\frac{2}{3}},\tau=\sqrt{a^3 v}g(\eta),\theta(\eta)=\frac{T-T_W}{T_W-T_\infty},\\&\phi(\eta)=\frac{C-C_w}{C_\infty},\chi(\eta)=\frac{N-N_W}{N_W-N_\infty}.\end{aligned}\right\} \tag{2.9}$$

$$g=f''\frac{g^2+A\gamma^2}{g^2+\gamma^2}, \tag{2.10}$$

$$g'=\frac{1}{3}f'^2-\frac{2}{3}ff''-Mf'+Gr(\theta-Nr\phi-Rb\chi)=0 \tag{2.11}$$

$$\left[1+\frac{4}{3}Rd\left\{1+\left(\theta_w-1\right)\theta\right\}^3\right]\theta''+4Rd\left(\theta_w-1\right)\left[1+\left(\theta_w-1\right)\theta\right]^2\theta'^2 + Pr\left[f\theta'+Nb\theta'\phi'+Nt\left(\theta'\right)^2\right]=0, \tag{2.12}$$

$$\phi''+LePrf\phi'+\frac{Nt}{Nb}\theta''-PrLe\sigma(1+\delta\theta)^n\exp\left(\frac{-E}{1+\delta 0}\right)\phi=0 \tag{2.13}$$

$$\chi''+Lbf\chi'-Pe\left[\phi''\left(\chi+\delta_1\right)+\chi'\phi'\right]=0, \tag{2.14}$$

$$\left.\begin{aligned}&f(0)=0,f'(0)=1+\Omega_1 f''(0)+\Omega_2 f'''(0),\theta'(0)=-Bi(1-\theta(0)),\\&\phi'(0)+\frac{Nt}{Nb}\theta'(0)=0,\chi(0)=1\\&f'(\infty)\to 0,\theta(\infty)\to 0,\phi(\infty)\to 0,\chi(\infty)\to 0.\end{aligned}\right\}$$

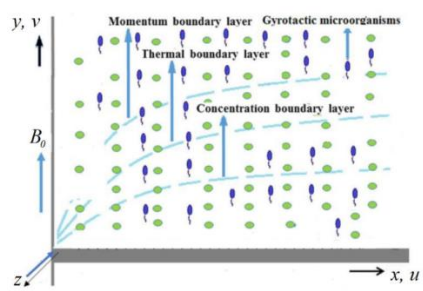

fig. A. Geometrical configurations of the two-dimensional nanofluid flow through stretching surface.

The buoyancy ratio parameter Nr is (CwCw) (pf) (1Cf) T if the fluid parameter A is equal to zero. Brownian constant Nb = (c)p DB (cw c) (c)f, Bingham number = S a 3, Bioconvection Rayleigh number Rb = (mf) (NwN) (1Cf) T, Mixed convection parameter = (1Cf) Prandtl number P r = f (TwoT) Aw, c'mon. parameter N t is the thermophoresis constant, which is equal to (c)p (Tw Tw)/fT. The activation energy E is equal to (c)p k1t, the chemical reaction parameter an is Kr2a and the temperature difference parameter is Tw/Tw/Tw. Dm is the Lewis number, 1 is the microorganism difference parameter Nw, and Peclet number P e is bw. There are three numbers that are displayed in this way: the local Nusselt number, the local Sherwood number, and the local motile density number :

$$\left.\begin{aligned} Sh\left(\mathrm{Re}_x\right)^{-0.5} &= -\phi'(0), \\ Nu\left(\mathrm{Re}_x\right)^{-0.5} &= -\left(1+\frac{4}{3}Rd\left(1+\left(\theta_w-1\right)\theta(0)\right)^3\right)\theta'(0), \\ Nn\left(\mathrm{Re}_x\right)^{-0.5} &= -\chi'(0). \end{aligned}\right\} \tag{2.16}$$

Numerical scheme

An approximation of the solution to flow equations is obtained using a numerical approach. The shooting technique is used to follow the numerical treatment with the assistance of MATLAB computational programme. After correct adjustments, the starting value system may be attained. Several iterations are necessary to get the desired level of precision. To begin the process, the following estimations are recommended:

$$\begin{aligned} & f = l_1, f' = l_2, f'' = l_3, f''' = l_3', \\ & \theta = l_4, \theta' = l_5, \theta'' = l_5', \\ & \phi = l_6, \phi' = l_7, \phi'' = l_7', \\ & \chi = l_8, \chi' = l_9, \chi'' = l_9', \end{aligned}$$

$$\left.\begin{aligned} l_3' &= \frac{1}{3}l_2^2 - \frac{2}{3}l_1 l_2^2 + Gr\left(l_4 - Nrl_6 - Ncl_8\right), \\ l_5' &= -\frac{Pr\left(l_1 l_5 + Ntl_5^2 + Nbl_5 l_7\right) + 4Rd\left(\theta_w-1\right)\left(1+\left(\theta_w-1\right)l_4\right)^2 l_5^2}{1+\left(\frac{4}{3}\right)Rd\left(1+\left(\theta_w-1\right)l_4\right)^3}, \\ l_7' &= -Scl_1 l_7 - \frac{Nt}{Nb}l_5' + Sc\sigma^{**}\left(1+\delta l_4\right)^n l_6 exp\left(\frac{-E}{1+\delta l_4}\right), \\ l_9' &= l_7 l_9 - Lbl_1 l_9 + Pe\left(l_8+\varpi\right)l_7'. \end{aligned}\right\} \tag{3.2}$$

with

$$\left.\begin{aligned} & l_1(0) = 0, l_2(0) = 1 + \gamma_1 l_3(0) + \gamma_2 l_{33}'(0), q_5(0) = -Bi\left(1 - l_4(0)\right), \\ & l_7(0) + \frac{Nt}{Nb}l_5(0) = 0, l_8(0) = 1, \\ & l_2(\infty) \to 0, l_4(\infty) \to 0, l_6(\infty) \to 0, l_8(\infty) \to 0. \end{aligned}\right\} \tag{3.3}$$

Physical analysis of results

The non-dimensional profile of velocity f ′, temperature, concentration, and the microbiological profile are used to physically check the flow parameter's governing physical mechanism. A number of flow parameters such as Bingham number, Prandtl number P, mixed convection parameter Gr and slip parameters parameter (1 and 2) are graphically depicted in order to show the influence of these flow parameters on the overall flow dynamics of the system. This includes the impact of all of these flow parameters on the overall flow dynamics of the system. For example, the impact of all of these flow parameters on the overall flow dynamics of the system is illustrated in this way. A = 0.2, Nr = 0.4, =0.2, Nb = 0.3, Pr = 1 and Rb = 0.5-0.5-0.5-0.5-0.5-0.5-0.5-0.5-0.5-0.5-0.5-0.5-0.5-0.5-0.5-0.5-0.5-0.5-0.5-0.5-0.5-0.5-0.5-0.5-0.5-0.5-0.5-0.5-0.5-0.5-0.5-0.5-0.5-0 See how the Philippoff fluid parameter A and slip parameter 1 affect f' in Figure 1 (click for larger version) (a). When A reaches its maximum value, a boost-up effect in velocity may be seen. As a result, leading values of 1 show a decreasing profile. The slip mechanism may be used to efficiently regulate the flow of fluid. Figure 1 shows the results of the function f ′ when the bioconvection Rayleigh number Rb and the second-order slip constant 2 vary (b). Application of both factors causes a decrease in f'. The decrease in f ′ due to Rb is related to buoyancy forces in a physical sense.

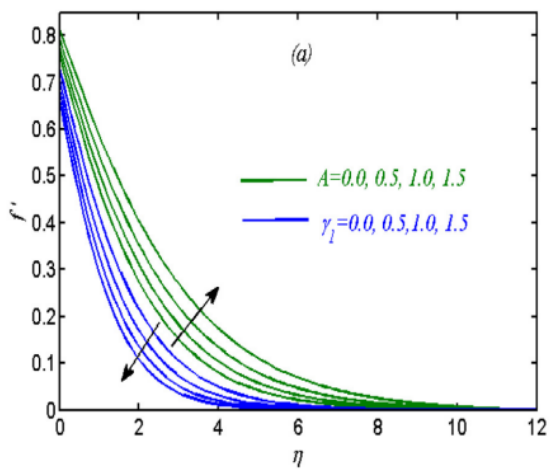

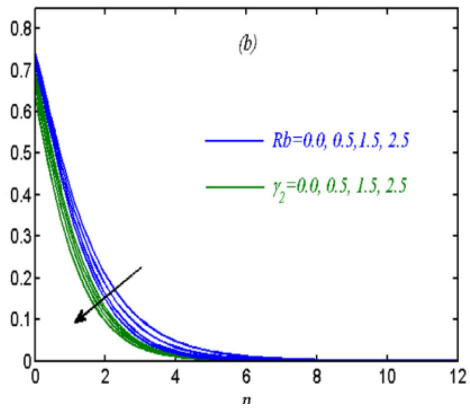

Fig. 1. (a) Change in $f\,'$ due to A and $\gamma 1$, (b) change in $f\,'$ due to Rb and $\gamma 2$

This slowed the entrance of blood. Similarly, the fluid particle resistance is increased by the second-order slip parameter, resulting in a decreasing profile. The graphs in Fig. 2(a–d) showed that the temperature profile of the nanofluid changed with various parameters. Drawing Fig. 2 indicates the significance of slip parameters 1 and 2 on (a). The temperature of nanofluids may be improved by using higher-order slip processes. Both parameters have an increasing effect on, although the shift is more gradual in the case of 1. To understand the effects of the Philippoff fluid parameter A and thermophoresis constant N t, go no further than figure 2(b). The temperature of the nanofluids lowers and increases with a change in A and N t. The migratory pattern of heated nanofluids in the cooler surface owing to temperature gradient is connected to the increasing contribution in due to thermophoresis factors. In Fig. 2(c), the significances of Bi and Nb on are included into the graphical analysis. A change in has been seen when Bi and Nb levels are altered. The effects of the radiation constant Rd and the surface heating constant w on nanofluid temperature are shown in Fig. 2(d). Due to both characteristics, a maximum change in is preferred. Due to the maximum fluctuation of Philippoff fluid parameter A and thermophoresis parameter N t, Fig. 3(a) shows a changed concentration profile. As N t changes, the amount of nanofluid in the solution increases. The thermophoresis phenomena has been interpreted as a physical explanation for the increased concentration of nanofluid, although the change in A has lowered the concentration profile. In Fig. 3, two key slip factors, 1 and 2, are shown to influence (b). Slip parameters have been shown to benefit mass transit by improving the profile. Fig. 3(c) shows that the concentration of nanofluids increases with the use of activation energy and magnetic force. The Lorentz force properties of the magnetic force were used to enhance mass transportation. Figure 4(a) depicts a graphical representation of the profile of a motile microorganism with real-world slip parameter values 1. Both slip variables have a significant effect on the motile bacteria profile. In this case, the difference owing to 2 is far greater. Fig. 4(b) shows how a numerical change in Peclet number P e and the Philippoff fluid parameter A affects the assessment of. The numerical values of P e are used to express the decreasing change in. Peclet number is reversely piggybacked with motile density, which is the physical explanation for such a depressed microbe profile. Table 1 is what you're looking at. For A, Nr, and N, the numerical assessment of f $''(0)$

A	Nr	Nc	$-f''(0)$
0.2	0.3	0.3	0.38598
0.4			0.350254
0.8			0.31785
0.3	0.2		0.3959
	0.6		0.41248
	1.0		0.43359
	0.2	0.2	0.43021
		0.5	0.44784
		0.9	0.45581

Table 2 Numerical treatment of $-\theta\,'(0)$ against flow parameter.

Pr	A	Nr	Nc	Rd	Nb	Nt	$-\theta'(0)$
0.2	1.0	0.2	0.2	0.4	0.2	0.3	0.49638
0.6							0.54858
1.0							0.59765
0.3	0.2	0.2	0.2	0.4	0.2	0.3	0.39877
	0.4						0.36301
	0.8						0.34543
2.0	1.0	0.1	0.2	0.4	0.2	0.3	0.4365
		0.5					0.41566
		0.9					0.40365
2.0	1.0	0.2	0.3	0.4	0.2	0.3	0.43753
			0.7				0.42754
			1.3				0.41743
2.0	1.0	0.2	0.2	0.3	0.2	0.3	0.45325
				0.5			0.42987
				0.9			0.39359
2.0	1.0	0.2	0.2	0.4	0.3	0.3	0.41748
					0.5		0.40257
					0.7		0.39867
2.0	1.0	0.2	0.2	0.4	0.2	0.1	0.547875
						0.5	0.52525
						0.9	0.47268

When the Philippoff fluid parameter A is at its maximum, rises. Table 1 shows the change in f $''(0)$ as a result of changes in A, Nr, and Nc. f $''(0)$ with A shows a diminishing numerical variation. While this is going on, fewer and fewer results are coming in.

Conclusions

Numerical simulations have shown that the gyrotactic microorganisms in Reiner–Philippoff nanofluid may be detected in this continuation. The nonlinear formulation of thermal radiation is also used. i. An increased change in velocity is calculated owing to greater values of the Philippoff fluid parameter. When attempting to regulate fluid velocity, slip parameters perform better than other methods. It takes longer for the temperature of nanofluids to rise with nonlinear radiation parameters. iv. The nanofluid temperature is successfully improved by considering slip effects in the radiative thermal flow issue.

References

1. Choi SU, Eastman JA. Enhancing Thermal Conductivity of Fluids with Nanoparticles. IL, United States: Argonne National Lab.; 1995.

2. Buongiorno J. Convective transport in nanofluids. J Heat Transf. 2006;128(3):240– 250.

3. Chakraborty T, Das K, Kundu PK. Analytical approach to a Jeffrey nanofluid flow towards a stagnation point coexisting with magnetic field and melting heat effects. J Mol Liq. 2017;229(1):443–452. http://dx.doi.org/10.1016/j.molliq.2016.12.078.

4. Hsiao KL. Stagnation electrical MHD nanofluid mixed convection with slip boundary on a stretching sheet. Appl Therm Eng. 2016;98:850–861. http://dx.doi. org/10.1016/j.applthermaleng.2015.12.138.

5. Gul A, Khan I, Makhanov SS. Entropy generation in a mixed convection Poiseulle flow of molybdenum disulphide Jeffrey nanofluid. Results Phys..2018;9:947–954.

6. Ahmed SE, Raizah ZA, Aly AM. Entropy generation due to mixed convection over vertical permeable cylinders using nanofluids. J King Saud Univ Sci. 2019;31(3):352–361. http://dx.doi.org/10.1016/j.jksus.2017.07.010.

7. Qayyum S, Khan MI, Hayat T, Alsaedi A, Tamoor M. Entropy generation in dissipative flow of Williamson fluid between two rotating disks. Int J Heat Mass Transfer. 2018;127:933–942. http://dx.doi.org/10.1016/j.ijheatmasstransfer.2018. 08.034.

8. Turkyilmazoglu M. Mixed convection flow of magnetohydrodynamic micropolar fluid due to a porous heated/cooled deformable plate: Exact solutions. Int J Heat Mass Transfer. 2017;106:127–134. http://dx.doi.org/10.1016/j.ijheatmasstransfer. 2016.10.056.

9. Eid MR, Mabood F, Mahny KL. On 3D Prandtl nanofluid flow with higherorder chemical reaction. Proc Inst Mech Eng C. 2020:0954406220975429,

10. Rashidi MM, Freidoonimehr N, Hosseini A, Bég OA, Hung TK. Homotopy simulation of nanofluid dynamics from a non-

linearly stretching isothermal permeable sheet with transpiration. Meccanica. 2014;49(2):469–482. http://dx.doi.org/10. 1007/s11012-013-9805-9.

11. Alaidrous AA, Eid MR. 3-D electromagnetic radiative non-Newtonian nanofluid flow with Joule heating and higher-order reactions in porous materials. Sci. Rep.. 2020;10(1):1–9.

12. Ibrahim W. Magnetohydrodynamics (MHD) flow of a tangent hyperbolic fluid with nanoparticles past a stretching sheet with second order slip and convective boundary condition. Results Phys..2017;7:3723–3731. http://dx.doi.org/10.1016/ j.rinp.2017.09.041.

13. Khan AS, Nie Y, Shah Z, et al. Influence of interfacial electrokinetic on MHD radiative nanofluid flow in a permeable microchannel with Brownian motion and thermophoresis effects. Open Phys. 2020;18(1):726–737. http://dx.doi.org/10. 1515/phys-2020-0161.

14. Waqas H, Imran M, Khan SU, Shehzad SA, Meraj MA. Slip flow of Maxwell viscoelasticity-based micropolar nanoparticles with porous medium: A numerical study. Appl Math Mech. 2019;40(9):1255–1268. http://dx.doi.org/10.1007/ s10483-019-2518-9.

15. Adesanya SO, Onanaye AS, Adeyemi OG, Rahimi-Gorji, Ibrahim M. Alarifi M. Evaluation of heat irreversibility in couple stress falling liquid films along heated inclined substrate. J Clean Prod. 2019;239:117608. http://dx.doi.org/10.1016/j. jclepro.2019.117608.

16. Seikh A, Akinshilo A, Taheri MH, et al. Influence of the nanoparticles and uniform magnetic field on the slip blood flows in arterial vessels. Phys. Scr.. 2019;49(12):125218

17. Mahanthesh B, Animasaun IL, Rahimi-Gorji M, Alarifi IM. Quadratic convective transport of dusty Casson and dusty Carreau fluids past a stretched surface with nonlinear thermal radiation, convective condition and non-uniform heat source/sink. Physica A. 2019;535:122471. http://dx.doi.org/10.1016/j.physa. 2019.122471. 18. Kuznetsov AV. Thermo-bioconvection in a suspension of oxytactic bacteria. Int Commun Heat Mass Transfer. 2005;32(8):991–999. http://dx.doi.org/10.1016/j. icheatmasstransfer.2004.11.005.

19. Khan WA, Rashad AM, Abdou MM, Tlili I. Natural bioconvection flow of a nanofluid containing gyrotactic microorganisms about a truncated cone. Eur J Mech B Fluids. 2019;75:133–142. http://dx.doi.org/10.1016/j.euromechflu.2019. 01.002.

20. Alhussain ZA, Renuka A, Muthtamilselvan M. A magneto-bioconvective and thermal conductivity enhancement in nanofluid flow containing gyrotactic microorganism. Case Stud Therm Eng. 2021;23:100809. http://dx.doi.org/10.1016/j. csite.2020.100